Growth Control of High-Performance InAs/GaSb Type-Ⅱ Superlattices via Optimizing the In/Ga Beam-Equivalent Pressure Ratio *

Da-Hong Su(苏大鸿)[1,2,3], Yun Xu(徐云)[1,2,3**], Wen-Xin Wang(王文新)[2,4], Guo-Feng Song(宋国峰)[1,2,3]

[1]*Institute of Semiconductors, Chinese Academy of Sciences, Beijing 100083*

[2]*College of Materials Science and Opto-Electronic Technology, University of Chinese Academy of Sciences, Beijing 100049*

[3]*Beijing Key Laboratory of Inorganic Stretchable and Flexible Information Technology, Beijing 100083*

[4]*Institute of Physics, Chinese Academy of Sciences, Beijing 100190*

(Received 22 November 2019)

The performance of type-Ⅱ superlattice (T2SL) long-wavelength infrared devices is limited by crystalline quality of T2SLs. We optimize the process of growing molecular beam epitaxy deposition T2SL epi-layers on GaSb (100) to improve the material properties. Samples with identical structure but diverse In/Ga beam-equivalent pressure (BEP) ratio are studied by various methods, including high-resolution x-ray diffraction, atomic force microscopy and high-resolution transmission electron microscopy. We find that appropriately increasing the In/Ga BEP ratio contributes to improving the quality of T2SLs, but too large In BEP will much more easily cause a local strain, which can lead to more InSb islands in the InSb interfaces. The InSb islands melt in the InSb interfaces caused by the change of chemical potential of In atoms may result in the "nail" defects covering the whole T2SLs, especially the interfaces of GaSb-on-InAs. When the In/Ga BEP ratio is about 1, the T2SL material possesses a lower full width at half maximum of +1 first-order satellite peak, much smoother surface and excellently larger area uniformity.

PACS: 73.21.Cd, 73.21.Ac, 73.61.Ey, 73.63.Hs DOI: 10.1088/0256-307X/37/3/037301

Since they were first presented by Sai-Halasz in 1977,[1] type-Ⅱ superlattices (T2SL) have received interest from researchers because they promise to be an excellent material system for infrared photodetectors.[2–5] Compared with other material systems, T2SL materials have many advantages such as unique band structure engineering, suppressed Auger recombination,[6] excellent spatial uniformity,[7] large electron effective mass, and covering 3 μm to 30 μm.[8–12] Recently, the T2SL long-wavelength infrared (LWIR) infrared focal plane array (FPA) has been developed, and significant progress in device performance, closing to the one of the $Hg_{1-x}Cd_xTe$ FPAs.[13,14]

Although InAs/GaSb T2SL infrared detectors have achieved a competitive performance, the state-of-the-art efficiency is still far away from its optimal one. To further improve device performances, some strategies, which include designing and preparing new T2SL materials,[15,16] developing novel structures,[5,17,18] optimizing device preparation,[2,16,19] and enhancing packaging technologies,[11] have been proposed. Particularly, enhancement of the crystalline quality of T2SL materials plays a pivotal role among these approaches. It is generally accepted that less defect density in high-quality T2SL materials possesses the longer minority carrier lifetime due to suppressing the Shockley-Read-Hall (SRH) recombination.[20–22] Furthermore, much work so far has focused on the growth temperature, the V/Ⅲ beam-equivalent pressure (BEP) ratio and the Sb/As BEP ratio to gain the preferable interface between the InAs and GaSb layers, thus accomplishing high-quality InAs/GaSb T2SL materials.[23–26] It is noteworthy that only very little investigation on optimizing the In/Ga BEP ratio has been employed in pursuit of the preferential InAs/GaSb T2SL interface.

In this work, we demonstrate that high-quality InAs/GaSb T2SL materials could be achieved by the optimization of the In/Ga BEP ratio in the process of growth. We perform comprehensive analyses of nail defects corresponding to InAs/GaSb T2SL materials prepared in different In/Ga BEP ratios using the high-resolution x-ray diffraction (HRXRD), the atomic force microscopy (AFM) and the high-resolution transmission electron microscopy (HRTEM). Probing the interplay between the morphology and the defects enables us to improve the understanding of the role of In/Ga BEP ratios in the preparation of InAs/GaSb T2SLs and helps to yield high-quality materials.

In our experiment, the InAs/GaSb T2SL materials were grown on n-type epi-ready GaSb(001) substrates by an RIBER 412 molecular beam epitaxy (MBE) system, which was equipped with dual-filament Knudsen cells for Ⅲ elemental solid sources of Ga and In and valved cracker cells for both As and Sb. The temper-

*Supported by the National Key Research and Development Program of China (Grant Nos. 2016YFB0402402 and 2016YFB0400601), the National Basic Research Program of China (Grant No. 2015CB351902), the National Science and Technology Major Project (2018ZX01005101-010), the National Natural Science Foundation of China (Grant Nos. 61835011 and U1431231), the Key Research Projects of the Frontier Science of the Chinese Academy of Sciences (Grant No. QYZDY-SSW-JSC004), and the Beijing Science and Technology Projects (Grant No. Z151100001615042).

**Corresponding author. Email: xuyun@semi.ac.cn

© 2020 Chinese Physical Society and IOP Publishing Ltd

atures of As and Sb cracking zones were set at 850℃ and 800℃, respectively, resulting in the most of V fluxes comprised of As_2 and Sb_2. Firstly, a 0.5 μm GaSb buffer was grown at 530℃. Then 100 periods of superlattices (SL), a period incorporated with 12 monolayers (MLs) of InAs and 7 MLs of GaSb, were doped at 390℃. The V/Ⅲ BEP ratio was set at 4 for both InAs and GaSb except sample D whose V/Ⅲ BEP ratio was set at 4 for both InAs and InSb. The valve of As cell was kept to be close except we needed to grow InAs layers to control the As-background pressure for Gasb layers and interface layers. In previous research, InSb interface layers were beneficial for the optical quality.[27,28] As a result all the interface layers of SLs were InSb forced interfaces in order to balance the stress, by a special shutter sequence. The GaSb growth rate was kept to be constant (0.5 ML/s), corresponding to Ga BEP of 4.5×10^{-7} Torr, and changed InAs growth rate as 0.2 ML/s, 0.3 ML/s and 0.4 ML/s, corresponding In BEP of 2.7×10^{-7}, 4.1×10^{-7}, 6.7×10^{-7} Torr, respectively. The more growth details are shown in Table 1.

Table 1. The growth details of four samples.

Sample	Ga flux (Torr)	Sb flux (Torr)	In flux (Torr)	As flux (Torr)	In/Ga BEP
A	4.5×10^{-7}	1.8×10^{-6}	2.7×10^{-7}	1.1×10^{-6}	0.5
B	4.5×10^{-7}	1.8×10^{-6}	4.1×10^{-7}	1.6×10^{-6}	0.9
C	4.5×10^{-7}	1.8×10^{-6}	6.7×10^{-7}	2.7×10^{-6}	1.5
D	4.5×10^{-7}	2.7×10^{-6}	6.7×10^{-7}	2.7×10^{-6}	1.5

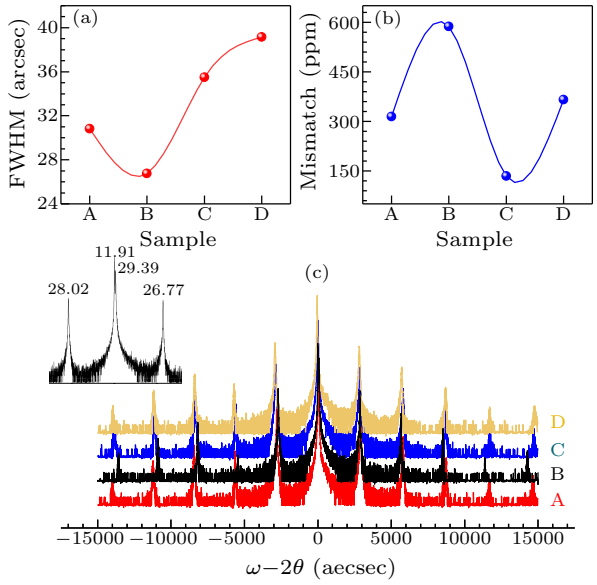

Fig. 1. (a) FWHM of +1 first-order satellite peak of the samples, (b) lattice mismatch of the samples, (c) high-resolution x-ray diffraction (HRXRD) for the samples.

The quality of samples was described by the Jordan valley high-resolution x-ray diffraction. As shown in Fig. 1(a), each sample's full width at half maximum (FWHM) of the first-order satellite peak is below 40 arcsec. The lattice mismatch of every sample is below 600 ppm from Fig. 1(b), which means that the strain of the whole structure is almost balanced. Figure 1(c) illustrates that the x-ray diffraction curves of all the samples have a large number of diffraction satellites, which indicate a favorable quality of samples. Compared the curves of Fig. 1(a) with Fig. 1(b), although sample B has a bigger mismatch 590.3 ppm, it still possesses the lowest FWHM of +1 first-order satellite peak (26.77 arcsec, which is shown on the top left corner of Fig. 1(c)). It can be seen that a higher growth rate is propitious to the quality of SL materials, which is consistent with the previous report.[28] However, if continue increasing the growth rate of InAs, the materials quality will be inhibited. At this stage, it can be guessed that this phenomenon may be caused by too high In BEP, leading some In atoms gathered on the interface.

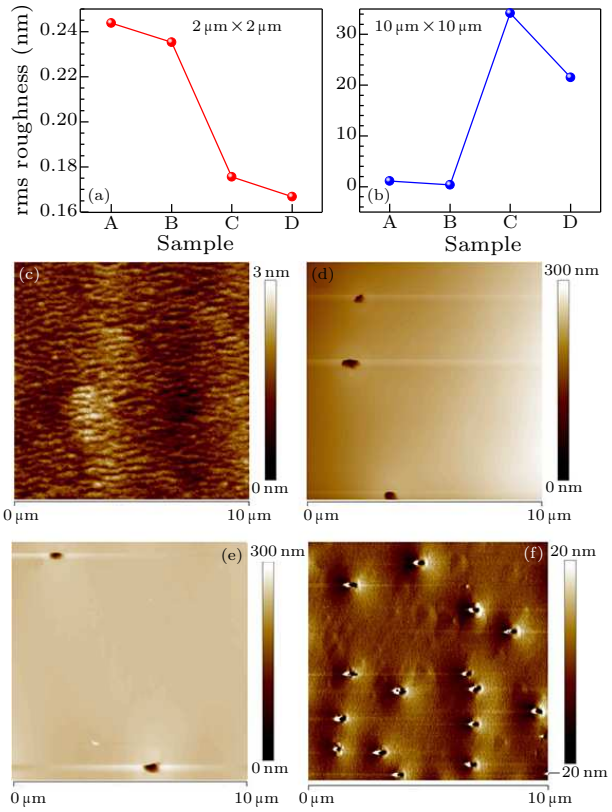

Fig. 2. (a) The rms roughness for $2 \times 2\,\mu m^2$ scans, (b) the rms roughness for $10 \times 10\,\mu m^2$ area, (c) the AFM image of $10 \times 10\,\mu m^2$ for sample B, (d) the AFM image of $10 \times 10\,\mu m^2$ for sample C, (e) the AFM image of $10 \times 10\,\mu m^2$ for sample D, (f) the AFM image of $30 \times 30\,\mu m^2$ for sample C.

We obtain the rms roughness of a $2 \times 2\,\mu m^2$ area for samples A, B, C and D all below 0.3 nm, which signifies the roughness of elevation is under one layer.

This result well accounts for the consequence of the FWHM of first-order satellite peak. All of the samples have a smooth surface in a relatively small area from the curve in Fig. 2.(a). However, the results of the samples are dramatically different, with a view to a lager region. The values of rms roughness over a $10 \times 10\,\mu m^2$ area for samples A, B, C and D are 1.08 nm, 0.37 nm, 32.00 nm and 22 nm, respectively. Sample B exhibits the best homogeneity among the four samples, because its rms roughness only has little increase with the test area expanded. Clear atomic steps can be seen on the surfaces of sample B from Fig. 2(c). The AFM images of $10 \times 10\,\mu m^2$ for samples C and D are shown in Figs. 2(d) and 2(e). Obviously, the AFM image of sample D is very similar to sample C. However, the results of samples C and D are observably different from the data of the smaller region. There are a lot of very deep holes in the epitaxial layers resulting in this conspicuous difference. The depth of holes can reach 130 nm at least. This type of deep holes was not an idiographic phenomenon, but nearly outright covering the surface of sample C, as shown in Fig. 2(f). This type of defect, which looks like a "nail", may be caused by the local strains within the superlattices.[29]

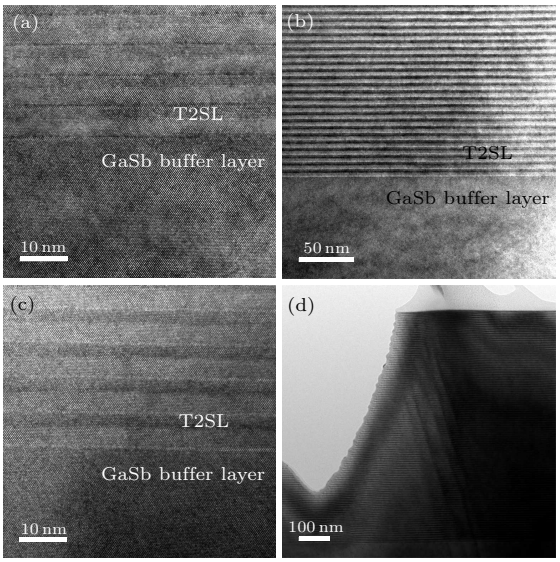

Fig. 3. (a) HRTEM image of sample B, (b) HRTEM image in larger scans area of sample B, (c) HRTEM images of sample C, (d) HRTEM image of the defect of sample C.

By the HRTEM images of sample B, the InAs/GaSb T2SLs have distinct and sharp boundaries, identical width of each layer, and less GaSb or InAs layer diffusing into the other layer. Meanwhile, there is no dislocation at all. Figure 3(c) shows an HRTEM image of the region far away from the defects of sample C. Although the boundaries are still distinct, it is more rough and tumble than sample B. There are several obvious dark-line defects, as displayed in Fig. 3(d). These defects originate from the interface of the T2SL-GaSb buffer layer, and the initial two thread-like defects continue on splitting during going through the whole T2SL layers.

The mismatch between InSb and GaSb is 7.8%, therefore the critical thickness is only one monolayer. The InSb islands were likely to be formed when the InSb interfaces were grown. The stress-strain relations can be written as[30]

$$\varepsilon_{ij} = \frac{1}{E}[(1+\nu) - \nu\delta_{ij}\sigma_{nn}], \tag{1}$$

where ε is indicative of the strain tensor, and E reveals the Young modulus, and σ is the stress, and ν exhibits the Poisson ratio. The stress-strain relations make the chemical potential of In atoms in InSb islands exhibit a difference.[31] When a thin GaSb layer is covered on the InSb islands, In atoms exit a thermodynamically favored tendency, will escape from the InSb islands and cover the free GaSb surface.[31] This thermodynamic process will increase confusion degree of the interface, especially the interfaces of GaSb on InAs. Even though the strain of the whole structure is balanced, there still exists a local strain area, especially in the interfaces of GaSb on InAs. With increasing thickness of T2SLs, this local strain may continue magnifying, leading to the nail defects.

In summary, we have reported the optimization of In/Ga BEP ratios during growth of InAs/GaSb T2SLs. The structure of 12 ML InAs and 7 ML GaSb T2SLs is studied by HRXRD, AFM and HRTEM. According to the results of these tests, when the In/Ga BEP ratio is about 1, the T2SL material possesses a lower FWHM of +1 first-order satellite peak, much smoother surface and excellently larger area uniformity. When the In/Ga BEP ratio is under 1, then fixing the GaSb growth rate, appropriately increasing the InAs growth rate can improve the quality of T2SLs. If continue increasing the In BEP, a local strain will occur much more easily, so that more InSb islands will be self-assembled in the interface. The InSb islands melt in the InSb interfaces caused by the change of chemical potential of In atoms may result in the nail defects covering the whole T2SLs, especially in the interfaces of GaSb on InAs.

References

[1] Sai-Halasz G A, Tsu R and Esaki L 1977 *Appl. Phys. Lett.* **30** 651
[2] Wei Y, Gin A, Razeghi M and Brown G J 2002 *Appl. Phys. Lett.* **80** 3262
[3] Johnson J L, Samoska L A, Gossard A C, Merz J L, Jack M D, Chapman G R, Baumgratz B A, Kasai K and Johnson S M 1996 *J. Appl. Phys.* **80** 1116
[4] Csuk R, Barthel A, Sczepek R, Siewert B and Schwarz S 1987 *J. Appl. Phys.* **62** 2545
[5] Aifer E H, Tischler J G, Warner J H, Vurgaftman I, Kim J C, Meyer J R, Bennett B R, Whitman L J, Jackson E M and Lorentzen J R 2005 *Proc. SPIE* **5732** 259
[6] Mohseni H, Litvinov V I and Razeghi M 1998 *Phys. Rev. B* **58** 15378
[7] Hao H Y, Wang G W, Wei X, Xi H, Xu Y Q, Liao Y Q, Yu Z, Ren Z W, Ni H Q and He Z H 2015 *Infrared Phys.* **72** 276

[8] Chen J, Xu Q, Zhou Y, Jin J, Lin C and He L 2011 *Nanoscale Res. Lett.* **6** 635
[9] Chen J, Yi Z, Xu Z, Xu J J, Chen Q Q, Chen H L and Li H 2013 *J. Cryst. Growth* **378** 596
[10] Chen X D, Cao X C, Liang Z, Zhang L X and He Y J 2016 *Opt. Quantum Electron.* **48** 84
[11] Rhiger D R, Bornfreund R E, Hill C J and Gunapala S D 2007 *Proc. SPIE* **6542** 654202
[12] Walther M, Schmitz J, Rehm R, Kopta S, Fuchs F, Fleißner J, Cabanski W and Ziegler J 2005 *J. Cryst. Growth* **278** 156
[13] Gunapala S D, Ting D Z, Hill C J, Soibel A and Rafol S B 2010 *Proc. SPIE* **7808** 780802
[14] Rhiger and David R 2011 *J. Electron. Mater.* **40** 1815
[15] Pullin M J, Hardaway H R, Heber J D and Phillips C C 1999 *Appl. Phys. Lett.* **75** 3437
[16] Rogalski A and Martyniuk P 2005 *Infrared Phys.* **48** 39
[17] Hoang A M, Chen G, Haddadi A, Pour S A and Razeghi M 2012 *Appl. Phys. Lett.* **100** 211101
[18] Jiang Z, Sun Y Y, Guo C Y, Lv Y X, Hao H Y, Jiang D W, Wang G W, Xu Y Q and Niu Z C 2019 *Chin. Phys. B* **28** 038504
[19] Rodriguez J B, Plis E, Bishop G, Sharma Y D, Kim H, Dawson L R and Krishna S 2007 *Appl. Phys. Lett.* **91** 043514
[20] Connelly B C, Metcalfe G D, Shen H and Wraback M 2010 *Appl. Phys. Lett.* **97** 251117
[21] Svensson S P, Donetsky D, Ding W, Maloney P and Belenky G 2009 *Appl. Phys. Lett.* **95** 1897
[22] Wang G W, Xu Y Q, Gao J, Tang B, Ren Z W, He Z H and Niu Z C 2010 *Chin. Phys. Lett.* **27** 077305
[23] Hua L I, Liu S, C E L L E K, Oray O, Ding D, S H E N, Xiao M, Steenbergen, Elizabeth H and Fan J 2013 *J. Cryst. Growth* **378** 145
[24] Jackson E M, Boishin G I, Aifer E H, Bennett B R and Whitman L J 2004 *J. Cryst. Growth* **270** 301
[25] Yu H L, Wu H Y, Zhu H J, Song G F and Xu Y 2016 *Chin. Phys. Lett.* **33** 128103
[26] Zhang Y, Ma W Q, Cao Y L, Huang J L, Yang W, Kai C and Shao J 2011 *IEEE J. Quantum Electron.* **47** 1475
[27] Haugan H J, Grazulis L, Brown G J, Mahalingam K and Tomich D H 2004 *J. Cryst. Growth* **261** 471
[28] Haugan H J, Brown G J and Grazulis L 2011 *J. Vac. Sci. & Technol. B* **29** 03C101
[29] Klin O, Snapi N, Cohen Y and Weiss E 2015 *J. Cryst. Growth* **425** 54
[30] Grundmann M, Stier O and Bimberg D 1995 *Phys. Rev. B* **52** 11969
[31] Ledentsov N N, Shchukin V A, Grundmann M, Kirstatedter N, Böhrer J, Schmidt O, Bimberg D, Ustinov V M, Egorov A Y and Zhukov A E 1996 *Phys. Rev. B* **54** 8743